JACS Au
AN OPEN ACCESS JOURNAL OF THE AMERICAN CHEMICAL SOCIETY

pubs.acs.org/jacsau

Article

Dinitrogen Activation by Heteronuclear Bimetallic Cluster Anion FeV^- in the Gas Phase

Shihu Du,[⊥] Xuegang Liu,[⊥] Zhiling Liu, Gang Li, Hongjun Fan, Hua Xie,* and Ling Jiang*

Cite This: *JACS Au* 2023, 3, 1723−1727

Read Online

ACCESS | Metrics & More | Article Recommendations | Supporting Information

ABSTRACT: Nitrogen activation is a significant but difficult project in the chemical area. Photoelectron spectroscopy (PES) and calculated results are used to investigate the reaction mechanism of the heteronuclear bimetallic cluster FeV^- toward N_2 activation. The results clearly show that N_2 can be fully activated by FeV^- at room temperature, forming the $FeV(\mu_2\text{-}N)_2^-$ complex with the totally ruptured N≡N bond. Electronic structure analysis reveals that the activation of N_2 by FeV^- is achieved by the electron transfer of bimetallic atoms and electron back-donation to the metal core, which demonstrates that heteronuclear bimetallic anionic clusters are very important to nitrogen activation. This study provides important information for the rational design of synthetic ammonia catalysts.

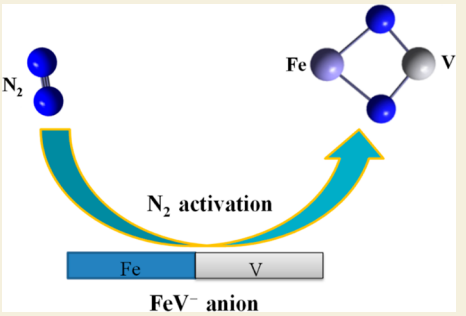

KEYWORDS: *nitrogen activation, synthetic ammonia catalysts, heteronuclear bimetallic anionic clusters, photoelectron spectroscopy, natural nitrogenases*

INTRODUCTION

The synthetic ammonia industry is crucial to fertilizer production and using NH_3 as an energy source.[1] Due to harsh conditions of the conventional Haber−Bosch industrial process, efficient transformation and activation of nitrogen under moderate conditions still maintain a great direction in the realm of chemical industry in which it has been actively aspired for over a century.[2−6] Natural nitrogenases are well known to be capable of activating N_2 in the atmospheric environment. Especially, iron−molybdenum nitrogenases have their activated locations of heteronuclear metals and are more effective than pure iron nitrogenases.[7−9] Given the polynuclear properties of active artificial sites and nitrogen fixation from biology, they are considerably vital to investigate metallic polynuclear nitrogen activation and fixation.[10−15]

In recent years, some condensed phase studies have demonstrated the synergism of heteronuclear metals in the N_2 activation via transferring electrons and lowering energy barriers. However, the selective assembly of the heteronuclear metal system still faces considerable challenges in the coacervation phase, which limits further investigations.[16] In contrast, isolated gaseous metal clusters can provide an ideal pattern to study bond activation processes without ambient interference.[17−19]

The reaction of N_2 and metal systems in the gaseous phase, containing pure metal complexes and clusters associated with various ligands (N, C, H, S, and others),[20,21] is studied in depth, as well as those between nitrogen clusters and metallic clusters. Nitrogen can be activated by transitional metallic nitrides like Ta_2N^+, $Ta_3N_3H_{0,1}^-$, $V_5N_5^-$, and so forth[20,22−24] and by the C−N coupling of $FeV_2C_2^-$, $FeTaC_2^-$, $Ta_2C_4^-$, $V_3C_4^-$, etc.[25−28] Additionally, the reaction of homonuclear metal species with nitrogen has been widely used as Ta_2^+, Ti_2, Gd_2, and so on.[29−31] Interestingly, there are similarities that nitrogen was activated in these studies. However, systematic studies on the reactivity of N_2 activation by heteronuclear bimetallic clusters remain scarce. Various metal cluster cations, anions, and atoms assimilate one or more N_2 to form physically adsorbed metal nitrogen complexes with relatively low activation of N_2. Studies on anion-mediated complete activation of N_2 in clusters including multiple atoms are scarce. Therefore, the study of the reaction between heteronuclear bimetal atoms and N_2 in a mild environment is of great significance for the activation of N_2 and identification of new reaction types. Given the significant character of vanadium and iron for activation and fixation of N_2, iron and vanadium were selected to react with nitrogen in this work. Notably, the complete breaking of the N≡N bond induced with the help of FeV^- was found by using photoelectron imaging spectroscopy combined with theoretical calculations.

Received: March 24, 2023
Revised: May 2, 2023
Accepted: May 3, 2023
Published: May 15, 2023

Experimental and Computational Methods

The photoelectron detachment experiments have been performed with our self-made instrument, which possesses a laser sputtering cluster ion source, a mass spectrometer with a double channel, and a photoelectron image spectrometer with a velocity map. Details of the experimental instrument can be found elsewhere.[32] By spraying helium gas with a pulsed laser, the FeV^- beam was generated. $FeVN_2^-$ clusters were obtained from the laser disintegration of the mixed metal target with 5% N_2 and 95% He. Their pressure for N_2 and He mixed gas was set as approximate 3 atm. The $FeVN_2^-$ anionic clusters were quickly cooled down and expanded in a laser ablation chamber. These clusters were further picked using a mass spectrometer from Wiley−McLaren. In the photodetachment of cluster anions, 532 or 1064 nm laser is acquired. Photoelectrons were recorded by a detector, which consisted of a phosphor screen and two micro-channel plates. In addition, two-dimensional (2D) photoelectron imaging results were acquired, which were normally recorded with a commercial charged coupling camera (CCD). Raw images were collected with 15,000 laser spots. It had a two-dimensional imaging detector, and the density of the photoelectron in its three-dimensional framework was projected onto this detector. The Abel Inverse Basis Set Expansion (BASEX) transformation method was applied to the initial three-dimensional distribution, and photoelectron spectra were acquired by reorganizing the corresponding three-dimensional images. The experimental results were corrected through the Au^- anion,[33] and the recorded energy resolution from the current instrument was more than 5%.

To elucidate the possible structures of the $FeVN_2^-$ anion, theoretical calculations at the BH&HLYP functional[34] level was carried out using the universal Gaussian 09.[35] The Def2-SVP basis set[34] was employed for all atoms. All possible electronic states were considered. To make sure that every structure on the potential energy surface has the actual minimum value, vibration analysis was performed. Theoretically, the difference for their energies from the anionic cluster and neutral species in an optimized anionic structure was set as vertical detachment energy (VDE). Additionally, the difference for their obtained energies from neutral species and corresponding anions in their respective optimized geometry is called adiabatic detachment energy (ADE). Relative energies embraced correction for zero-point energy. Combining the natural population analysis (NPA) and molecular orbital analyses to $FeVN_2^-$ was executed, and the natural bond orbital (NBO) 3.1 version was implemented.[36]

RESULTS AND DISCUSSION

The experimental imaging spectra of $FeVN_2^-$ recorded at 1064 or 532 nm are shown in Figure 1. This dominant peak (X) represents the VDE of its ground state for $FeVN_2^-$, and its value is directly estimated to be 0.75 ± 0.02 eV. The absence of vibrational details limits the direct measurement of its ADE, which is alternatively estimated to be 0.72 ± 0.02 eV by the connection of the horizontal axis with a rising edge of the ground-state band.

To obtain an in-depth molecular level understanding of the observed spectra, multiple optimized structures for $FeVN_2^-$ are theoretically located and alphabetically labeled from A to J according to the relative energies (Figure S1). According to the relative energies of these complexes, the most appropriate five low energy isomers (A−E) are selected as the research objects for discussion. In the lowest-lying isomer A, N_2 is completely cleaved and each N atom binds to both the Fe and V atoms, forming a quadrilateral C_{2v} configuration containing two V−N−Fe bridges with a $^7A_2$ ground state. Isomer B has 0.25 eV higher energy and a $^3A'$ state. C lies 0.80 eV higher compared to isomer A, and N_2 is terminally Fe atom. The fourth low energy structure D, which possesses nearly identical energy to isomer C, is the one in which the N_2 is completely split with a $^3A'$ state. Isomer E has 0.91 energy and exhibits a C_s configuration with a $^7A'$ state where N_2 binds to Fe in an end-to-end manner.

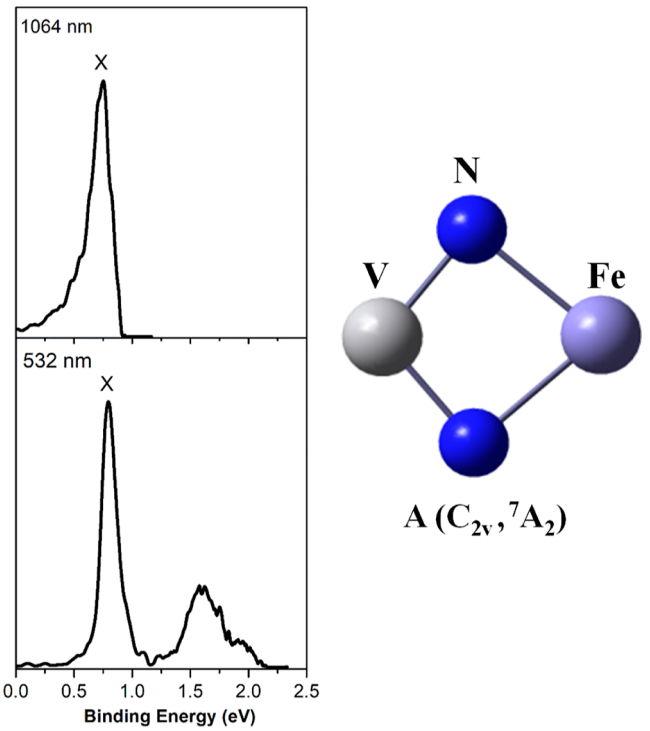

Figure 1. Photoelectron spectrum of $FeVN_2^-$ recorded at 532 nm (2.331 eV) and the corresponding observation at 1064 nm (1.165 eV). The lowest-lying isomer for $FeVN_2^-$ anion and its electronic state is given.

The experimental results of VDE/ADE values (Table 1) for the $FeVN_2^-$ anion are combined with the theoretical values for the obtained structures to promote the spectral assignments and structural identification. The theoretical VDE and ADE results for isomer A are 0.82/0.75 eV, which are in accordance with the experiment. In contrast, those values of isomer *B* equal to 1.16/0.94 eV are considerably higher. The computed results of the remaining isomers from C to E (0.42/0.32 eV,

Table 1. Experimental ADE and VDE Results Comparison to the Five Calculated Values at BH&HLYP for $FeVN_2^-$

			VDE (eV)		ADE (eV)	
cluster	isomer	relative energy (eV)	Expt[a]	Calc	Expt[a]	Calc
$FeVN_2^-$	A	0.00	0.75(2)	0.82	0.72(2)	0.75
	B	0.25		1.16		0.94
	C	0.80		0.42		0.32
	D	0.82		1.94		1.54
	E	0.91		1.36		0.89

[a]The numbers in parentheses stand for the experimental uncertainty.

https://doi.org/10.1021/jacsau.3c00143
JACS Au 2023, 3, 1723−1727

1.94/1.54 eV, and 1.36/0.89 eV), however, are even less consistent with the experimental results. Additional evidence provided by the simulated spectra as density-of-state (DOS) spectra, on the basis of the computed generalized Koopman theorem, is illustrated in Figure S2. The DOS spectrum of isomer A nicely reproduces the experimental result, while the other simulated DOS spectra exhibit huge differences. Consequently, isomer A is confirmed to be responsible for the experimental spectra.

The potential energy profile along with multiple intermediates and transition states are calculated to seek how isomer A is dynamically transformed from the isolated N_2 and FeV^- (Figure 2). To start with, one nitrogen approaches the

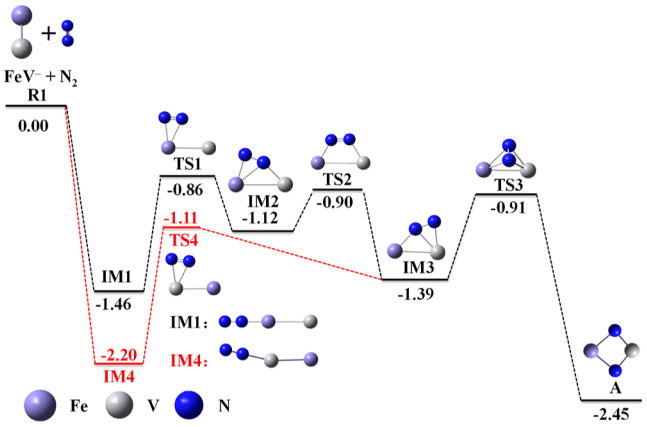

Figure 2. Theoretical potential energy profiles for the N_2 reaction with the FeV^- anion. The intermediates (IM1−IM4) and possible transition states (TS1−TS4) are revealed in eV after correction for zero-point energies.

iron from the opposite side of the V atom, forming a linear IM1 structure, which consumes 0.60 eV to be further converted to a side-on IM2 structure. Meanwhile, the N atom of IM1 gets close to the V atom for the V−N bond to come into being, then its bond length from N−N increases to 0.03 Å (Figure S3). From IM2 to IM3, its isomerization process can be found, and this suggests its rupture for the bond of Fe−N and the formation of another V−N bond. It can be found that this process needs an energy of about 0.22 eV. By comparison, the conversion from IM3 to A needs 0.48 eV to totally break the N−N bond. In addition, when the V atom acts as the adsorption site, the reaction pathway needs to conquer 1.09 eV from IM4 to TS4, which is approximately 0.5 eV higher than the process from IM1 to TS1. The energetics of TS1 and TS4 are highly lower than the initial reactants, suggesting that the two pathways involving Fe and V atoms as the adsorption sites are both feasible.

The molecular orbital analysis of TS3, as shown in Figure 3, supports the nitrogen activation mechanism. The HOMO-3 and HOMO-4 orbitals have a π-back-donation characteristic, which comes from the occupied 3d orbital of V and Fe into N_2.

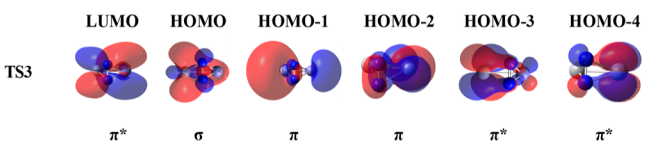

Figure 3. Molecular orbital pictures of TS3 for $FeVN_2^-$.

The previous results have indicated that the bond of N≡N can be lowered due to π-back-donation, which was suitable for the subsequent reaction activation process.[37] Compared with end-on structures, these side-on structures have a greater degree of activation. Noting the HOMO-3 of TS3 as a V−N π orbital, HOMO-4 can be viewed as a Fe−N σ orbital; both orbitals devote to weakening of the bond of N≡N. In transformation from the isolated N_2 and FeV group to the isomer A, the distance of the N−N bond is progressively extended to 1.44 Å. Interestingly, the Fe−V bond length gets longer from R1 to IM2, while it gets shorter from IM2 to A (Figure S3), implying transfers electrons of FeV^- to N_2 from R1 to IM2 while transfers electrons of N_2 to FeV^- from IM2 to A.

To visualize the charge variation among those involved atoms, NPA is performed (Figure 4), and we mainly discuss

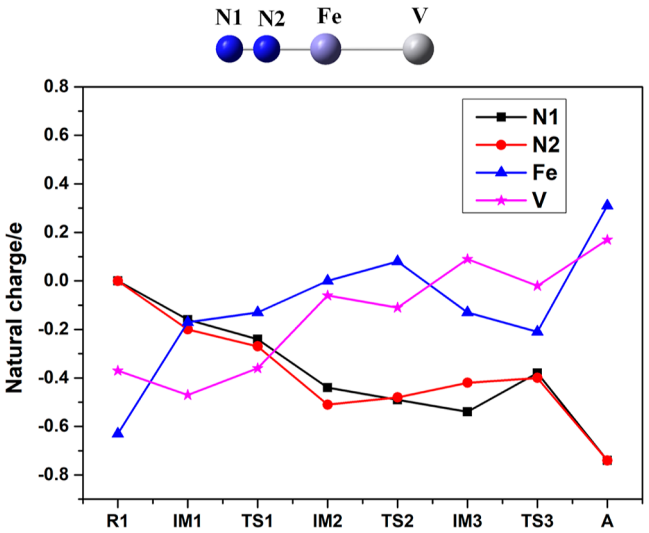

Figure 4. Natural population analysis (NPA) charge of $FeVN_2^-$.

the reaction pathway with Fe as the adsorption site. According to the natural charge trend, the transferring electron from FeV^- to N_2 induces the rupture of the N≡N bond. For FeV^-, the internal charge enriches Fe, thereby further enhancing its catalytic performance. The negative charge of Fe on FeV^- is transferred to the N_2 and V atoms when nitrogen is strapped to FeV^- (R1 to IM1). It reveals π-back-donation of the occupied 3d orbital for iron into the π^* orbital toward N_2 and is the key to the activity of reduced nitrogen. However, the negative charge of the nitrogen unit decreases with the negative charge on the two metal groups increasing to some extent from IM3 to TS3. It indicates that the electron return phenomenon promotes nitrogen activation from the N_2 to FeV group, and the experimental and theoretical evidence confirms that iron and vanadium atoms are quite significant in the activated reaction mechanism of N_2. Taken together, this study reveals the underlying mechanism of the electron back-donation of nitrogen to the metallic core at their reaction process.

CONCLUSIONS

In this work, the reaction between FeV^- and N_2 was investigated by combining photoelectron imaging spectroscopy and theoretical calculations, suggesting that FeV^- can effectively crack and activate N_2 at room temperature. The lowest-lying geometry of $FeVN_2^-$ possesses the FeV nitride with a ring configuration. Further calculations and analyses

https://doi.org/10.1021/jacsau.3c00143
JACS Au 2023, 3, 1723−1727

show that the catalytic process is enabled by the bimetallic electron transfer. In general, the bimetal charge transfer to nitrogen promotes nitrogen activation, and the electron return phenomenon is found in FeV^- cracking and activating the N_2 reaction. The underlying mechanism of nitrogen co-activation by heteronuclear bimetal atoms has been revealed, which is promising for the research and development of novel ammonia catalysts.

■ ASSOCIATED CONTENT

Supporting Information

The Supporting Information is available free of charge at https://pubs.acs.org/doi/10.1021/jacsau.3c00143.

Low energy isomers, simulated photoelectron spectra for the $FeVN_2^-$ anion, and potential energy profile for FeV^- with N_2 (PDF)

■ AUTHOR INFORMATION

Corresponding Authors

Hua Xie − *State Key Laboratory of Molecular Reaction Dynamics, Dalian Institute of Chemical Physics, Chinese Academy of Sciences, Dalian 116023, China;* orcid.org/0000-0003-2091-6457; Email: xiehua@dicp.ac.cn

Ling Jiang − *State Key Laboratory of Molecular Reaction Dynamics, Dalian Institute of Chemical Physics, Chinese Academy of Sciences, Dalian 116023, China;* orcid.org/0000-0002-8485-8893; Email: ljiang@dicp.ac.cn

Authors

Shihu Du − *State Key Laboratory of Molecular Reaction Dynamics, Dalian Institute of Chemical Physics, Chinese Academy of Sciences, Dalian 116023, China; School of Mathematics and Physics, Hebei University of Engineering, Handan 056038, China*

Xuegang Liu − *State Key Laboratory of Molecular Reaction Dynamics, Dalian Institute of Chemical Physics, Chinese Academy of Sciences, Dalian 116023, China; Center of Basic Molecular Science, Department of Chemistry, Tsinghua University, Beijing 100084, China*

Zhiling Liu − *School of Chemical and Material Science, Key Laboratory of Magnetic Molecules & Magnetic Information Materials, Ministry of Education, Shanxi Normal University, Taiyuan 030000, China;* orcid.org/0000-0002-1669-396X

Gang Li − *State Key Laboratory of Molecular Reaction Dynamics, Dalian Institute of Chemical Physics, Chinese Academy of Sciences, Dalian 116023, China;* orcid.org/0000-0001-5984-111X

Hongjun Fan − *State Key Laboratory of Molecular Reaction Dynamics, Dalian Institute of Chemical Physics, Chinese Academy of Sciences, Dalian 116023, China;* orcid.org/0000-0003-3406-6932

Complete contact information is available at: https://pubs.acs.org/10.1021/jacsau.3c00143

Author Contributions

⊥S.H.D. and X.G.L. shared the first authorship and contributed equally.

Notes

The authors declare no competing financial interest.

■ ACKNOWLEDGMENTS

The authors thank the Dalian Coherent Light Source (DCLS) for their help and support. The work has been well funded by the NSFC (Grant nos. 22273101, 22125303, 92061203, 22288201, and 21873097), the Youth Innovation Promotion Association from the Chinese Academy of Sciences (CAS) (2020187), the Dalian Young Star of Science and Technology Project (no. 2021RQ128), the Dalian Institute of Chemical Physics (DICP DCLS201702), the Strategic Priority Research Program of CAS (XDB17000000), the CAS (GJJSTD20190002), and the K. C. Wong Education Foundation (GJTD-2018-06).

■ REFERENCES

(1) Guo, J.; Chen, P. Catalyst: NH_3 as an Energy Carrier. *Chem* **2017**, *3*, 709−712.

(2) Yandulov, D. V.; Schrock, R. R. Catalytic Reduction of Dinitrogen to Ammonia at a Single Molybdenum Center. *Science* **2003**, *301*, 76−78.

(3) Weare, W. W.; Dai, X.; Byrnes, M. J.; Chin, J. M.; Schrock, R. R.; Muller, P. Catalytic reduction of dinitrogen to ammonia at a single molybdenum center. *Proc. Natl. Acad. Sci. U.S.A.* **2006**, *103*, 17099−17106.

(4) Erisman, J. W.; Sutton, M. A.; Galloway, J.; Klimont, Z.; Winiwarter, W. How a century of ammonia synthesis changed the world. *Nat. Geosci.* **2008**, *1*, 636−639.

(5) Wu, L. J.; Wang, Q.; Guo, J.; Wei, J.; Chen, P.; Xi, Z. From Dinitrogen to N-Containing Organic Compounds: Using Li_2CN_2 as a Synthon. *Angew. Chem., Int. Ed.* **2023**, *135*, No. e202219298.

(6) Anderson, J. S.; Rittle, J.; Peters, J. C. Catalytic conversion of nitrogen to ammonia by an iron model complex. *Nature* **2013**, *501*, 84−87.

(7) Zhao, Y.; Bian, S.; Zhou, H.; Huang, J. Diversity of Nitrogenase Systems in Diazotrophs. *J. Integr. Plant Biol.* **2006**, *48*, 745−755.

(8) Seefeldt, L. C.; Hoffman, B. M.; Peters, J. W.; Raugei, S.; Beratan, D. N.; Antony, E.; Dean, D. R. Energy Transduction in Nitrogenase. *Acc. Chem. Res.* **2018**, *51*, 2179−2186.

(9) Zhao, Y.; Bian, S.; Zhou, H.; Huang, J. Diversity of Nitrogenase Systems in Diazotrophs. *J. Integr. Plant Biol.* **2006**, *48*, 745−755.

(10) Clouston, L. J.; Bernales, V.; Carlson, R. K.; Gagliardi, L.; Lu, C. C. Bimetallic cobalt-dinitrogen complexes: impact of the supporting metal on N_2 activation. *Inorg. Chem.* **2015**, *54*, 9263−9270.

(11) Cammarota, R. C.; Clouston, L. J.; Lu, C. C. Leveraging molecular metal−support interactions for H_2 and N_2 activation. *Coord. Chem. Rev.* **2017**, *334*, 100−111.

(12) Martirez, J. M.; Carter, E. A. Excited-State N_2 Dissociation Pathway on Fe-Functionalized Au. *J. Am. Chem. Soc.* **2017**, *139*, 4390−4398.

(13) Ma, X. L.; Liu, J. C.; Xiao, H.; Li, J. Surface Single-Cluster Catalyst for N_2-to-NH_3 Thermal Conversion. *J. Am. Chem. Soc.* **2018**, *140*, 46−49.

(14) Ohki, Y.; Uchida, K.; Tada, M.; Cramer, R. E.; Ogura, T.; Ohta, T. N_2 activation on a molybdenum-titanium-sulfur cluster. *Nat. Commun.* **2018**, *9*, 3200.

(15) Zhang, N.; Jalil, A.; Wu, D.; Chen, S.; Liu, Y.; Gao, C.; Ye, W.; Qi, Z.; Ju, H.; Wang, C.; Wu, X.; Song, L.; Zhu, J.; Xiong, Y. Refining Defect States in $W_{18}O_{49}$ by Mo Doping: A Strategy for Tuning N_2 Activation towards Solar-Driven Nitrogen Fixation. *J. Am. Chem. Soc.* **2018**, *140*, 9434−9443.

(16) Collman, J. P.; Boulatov, R. Heterodinuclear Transition-Metal Complexes with Multiple Metal-Metal Bonds. *Angew. Chem., Int. Ed.* **2002**, *41*, 3948−3961.

(17) O'Hair, R. A. J.; Khairallah, G. N. Gas Phase Ion Chemistry of Transition Metal Clusters: Production, Reactivity, and Catalysis. *J. Clust. Sci.* **2004**, *15*, 331−363.

(18) Du, S. H.; Liu, X. G.; Ju, B. M.; Zhang, J. M.; Zou, J. H.; Li, G.; Fan, H. J.; Xie, H.; Jiang, L. Spectroscopic Identification of the Dinitrogen Fixation and Activation by Metal Carbide Cluster Anions PtC_n^- (n = 4-6). *Inorg. Chem.* **2023**, *62*, 170−177.
(19) Schwarz, H. Ménage-à-trois: single-atom catalysis, mass spectrometry, and computational chemistry. *Catal. Sci. Technol.* **2017**, *7*, 4302−4314.
(20) Sun, X. Y.; Zhou, S. Z.; Yue, L.; Guo, C.; Schlangen, M.; Schwarz, H. On the Remarkable Role of the Nitrogen Ligand in the Gas-Phase Redox Reaction of the N_2O/CO Couple Catalyzed by $[NbN]^+$. *Angew. Chem., Int. Ed.* **2019**, *58*, 3635−3639.
(21) Paul, M.; Detmar, E.; Schlangen, M.; Breugst, M.; Neudörfl, J.; Schwarz, H.; Berkessel, A.; Schäfer, M. Intermediates of N-Heterocyclic Carbene (NHC) Dimerization Probed in the Gas Phase by Ion Mobility Mass Spectrometry: C-H···C Hydrogen Bonding Versus Covalent Dimer Formation. *Chem. Eur. J.* **2019**, *25*, 2511−2518.
(22) Cheng, X.; Li, Z. Y.; Mou, L. H.; Ren, Y.; Liu, Q. Y.; Ding, X. L.; He, S. G. Side-on-End-on Coordination of Dinitrogen on a Polynuclear Vanadium Nitride Cluster Anion $[V_5N_5]^-$. *Chem. Eur. J.* **2019**, *25*, 16523−16527.
(23) Geng, C.; Li, J.; Weiske, T.; Schwarz, H. Complete cleavage of the N≡N identical withN triple bond by Ta_2N^+ via degenerate ligand exchange at ambient temperature: A perfect catalytic cycle. *Proc. Natl. Acad. Sci. U.S.A.* **2019**, *116*, 21416−21420.
(24) Zhao, Y.; Cui, J. T.; Wang, M.; Valdivielso, D. Y.; Fielicke, A.; Hu, L. R.; Cheng, X.; Liu, Q. Y.; Li, Z. Y.; He, S. G.; Ma, J. B. Dinitrogen Fixation and Reduction by $Ta_3N_3H_{0,1}^-$ Cluster Anions at Room Temperature: Hydrogen-Assisted Enhancement of Reactivity. *J. Am. Chem. Soc.* **2019**, *141*, 12592−12600.
(25) Li, Z. Y.; Mou, L. H.; Wei, G. P.; Ren, Y.; Zhang, M. Q.; Liu, Q. Y.; He, S. G. C.-N. Coupling in N_2 Fixation by the Ditantalum Carbide Cluster Anions $Ta_2C_4^-$. *Inorg. Chem.* **2019**, *58*, 4701−4705.
(26) Li, Z. Y.; Li, Y.; Mou, L. H.; Chen, J. J.; Liu, Q. Y.; He, S. G.; Chen, H. A Facile N identical withN Bond Cleavage by the Trinuclear Metal Center in Vanadium Carbide Cluster Anions $V_3C_4^-$. *J. Am. Chem. Soc.* **2020**, *142*, 10747−10754.
(27) Mou, L. H.; Li, Y.; Li, Z. Y.; Liu, Q. Y.; Ren, Y.; Chen, H.; He, S. G. Dinitrogen Activation and Functionalization by Heteronuclear Metal Cluster Anions $FeV_2C_2^-$ at Room Temperature. *J. Phys. Chem. Lett.* **2020**, *11*, 9990−9994.
(28) Mou, L. H.; Li, Y.; Li, Z. Y.; Liu, Q. Y.; Chen, H.; He, S. G. Dinitrogen Activation by Heteronuclear Metal Carbide Cluster Anions $FeTaC_2^-$: A 5d Early and 3d Late Transition Metal Strategy. *J. Am. Chem. Soc.* **2021**, *143*, 19224−19231.
(29) Himmel, H. J.; Hubner, O.; Klopper, W.; Manceron, L. Cleavage of the N_2 triple bond by the Ti dimer: a route to molecular materials for dinitrogen activation? *Angew. Chem., Int. Ed.* **2006**, *45*, 2799−2802.
(30) Zhou, M.; Jin, X.; Gong, Y.; Li, J. Remarkable dinitrogen activation and cleavage by the Gd dimer: from dinitrogen complexes to ring and cage nitrides. *Angew. Chem., Int. Ed.* **2007**, *46*, 2911−2914.
(31) Geng, C.; Li, J.; Weiske, T.; Schwarz, H. Ta_2^+-mediated ammonia synthesis from N_2 and H_2 at ambient temperature. *Proc. Natl. Acad. Sci. U.S.A.* **2018**, *115*, 11680−11687.
(32) Qin, Z. B.; Wu, X.; Tang, Z. C. Note: A novel dual-channel time-of-flight mass spectrometer for photoelectron imaging spectroscopy. *Rev. Sci. Instrum.* **2013**, *84*, 066108.
(33) Xie, H.; Zou, J. H.; Kong, X. T.; Zhang, W. Q.; Ahmed, M.; Jiang, L. Probing the microhydration of metal carbonyls: a photoelectron velocity-map imaging spectroscopic and theoretical study of $Ni(CO)_3(H_2O)_n^-$. *Phys. Chem. Chem. Phys.* **2016**, *18*, 26719−26724.
(34) Dunning, T. H. Gaussian basis sets for use in correlated molecular calculations. I. The atoms boron through neon and hydrogen. *J. Chem. Phys.* **1989**, *90*, 1007−1023.
(35) Frisch, M. J.; Trucks, G. W.; Schlegel, H. B.; Scuseria, G. E.; Robb, M. A.; Cheeseman, J. R.; Scalmani, G.; Barone, V.; Mennucci, B.; Petersson, G. A.; Nakatsuji, H.; Caricato, M.; Li, X.; Hratchian, H. P.; Izmaylov, A. F.; Bloino, J.; Zheng, G.; Sonnenberg, J. L.; Hada, M.; Ehara, M.; Toyota, K.; Fukuda, R.; Hasegawa, J.; Ishida, M.; Nakajima, T.; Honda, Y.; Kitao, O.; Nakai, H.; Vreven, T.; Montgomery, J. A., Jr.; Peralta, J. E.; Ogliaro, F.; Bearpark, M. J.; Heyd, J.; Brothers, E. N.; Kudin, K. N.; Staroverov, V. N.; Kobayashi, R.; Normand, J.; Raghavachari, K.; Rendell, A. P.; Burant, J. C.; Iyengar, S. S.; Tomasi, J.; Cossi, M.; Rega, N.; Millam, N. J.; Klene, M.; Knox, J. E.; Cross, J. B.; Bakken, V.; Adamo, C.; Jaramillo, J.; Gomperts, R.; Stratmann, R. E.; Yazyev, O.; Austin, A. J.; Cammi, R.; Pomelli, C.; Ochterski, J. W.; Martin, R. L.; Morokuma, K.; Zakrzewski, V. G.; Voth, G. A.; Salvador, P.; Dannenberg, J. J.; Dapprich, S.; Daniels, A. D.; Farkas, O.; Foresman, J. B.; Ortiz, J. V.; Cioslowski, J.; Fox, D. J. *Gaussian 09*; Gaussian, Inc.: Wallingford, CT, USA, 2009.
(36) Glendening, E. D.; Reed, A. E.; Carpenter, J. E.; Weinhold, F. *NBO 3.1*; Theoretical Chemistry Institute, 1998.
(37) Deng, G. H.; Pan, S.; Wang, G. J.; Zhao, L. L.; Zhou, M. F.; Frenking, G. Side-On Bonded Beryllium Dinitrogen Complexes. *Angew. Chem., Int. Ed.* **2020**, *59*, 10603−10609.

https://doi.org/10.1021/jacsau.3c00143
JACS Au 2023, 3, 1723−1727